| REV. | BY & DATE | DESCRIPTION | CHECK | APPROVED & DATE |
|---|---|---|---|---|
| Prepared by E.R. and J.G. | July 27, 2004 | On-ground calibration report for the GRNS/GRS instrument. | | |

**ADVISORY: This document has NOT been reviewed for export control and therefore may be subject to ITAR regulations or requirements.**

Ralph L. McNutt, Jr., Project Scientist and — Date 8/5/04

Robert Gold, Payload Manager — Date 7/29/04

Edgar Rhodes, Instrument Scientist — Date 7-29-04

William Boynton, Cognizant Co-Invetigator — Date 8/11/04

John Goldsten, Instrument Engineer — Date 8/9/04

Released — Date

| PART NUMBER | SIZE | NEXT ASSEMBLY | QTY./NA | USED ON | EFFECTIVITY - END ITEM SER. NO. | WEIGHT |
|---|---|---|---|---|---|---|
| | | | | | | |

THE JOHNS HOPKINS UNIVERSITY
APPLIED PHYSICS LABORATORY
11100 JOHNS HOPKINS ROAD, LAUREL, MARYLAND 20723-6099

# MESSENGER Gamma-Ray Spectrometer (GRNS/GRS) Calibration Report

| FSCM NO. | SIZE | DRAWING NO. | REV. |
|---|---|---|---|
| 88898 | A | 7384-9466 | A |

SCALE NONE | DO NOT SCALE PRINT | SHEET 1 OF 34

## Table of Contents

## EXECUTIVE SUMMARY

All necessary tests and calibrations have been conducted. Sufficient data has been analyzed to determine mission readiness. The measured differential and integral nonlinearity (INL) of the GRS are negligible and the INL temperature dependence is also negligible. Measured temperature coefficients indicate all gain drifts will lead to only small spectral thermal corrections. The measured Ge detector energy resolution over the energy range of interest during the spacecraft Comprehensive Performance Test was excellent, exceeding the 4 keV goal at 1332 keV by 0.5 keV. The functional test results also indicate more than adequate performance for the GRS to meet science mission requirements. The spacecraft GRS comprehensive performance test data uniformly exceeds the goals set for the GRS.

The GRS spatial calibration performed at the NIST cold-neutron-beam reactor holds the promise for a new higher level of calibration precision for this space-borne Ge gamma-ray spectrometer, while requiring far less total measurement time than needed for Ge spectrometers in previous missions. The efficiency calculation from the experimental data for the nadir-pointing case with no escapes is from 10% to 30% lower than that obtained from a Monte Carlo model used in CDR predictions of crust element sensitivity. However the basic CDR conclusions remain unchanged. Fe, Mg, Si, K, and Th should be mappable and Na and Ti should be measurable. The scientific objectives of the GRS component of the GRNS instrument are expected to be met and exceeded: (1) provide surface abundances of major elements, particularly those elements whose abundances are thought to be indicative of planetary evolution; (2) provide surface abundances of Fe, Si, and K and infer alkali depletion from K abundance; (3) map surface element abundances where possible, otherwise provide surface-averaged abundances or establish upper limits.

## INTRODUCTION

This report describes the ground calibration measurements performed and results and data analysis obtained up to the present time for the MESSENGER Gamma-ray Spectrometer (GRS), within the framework of the calibration plan. The focus is on verification of functionality and performance in meeting MESSENGER mission science objectives.

The scientific objectives of the GRS component of the GRNS instrument are to:

(1) provide surface abundances of major elements, particularly those elements whose abundances are thought to be indicative of planetary evolution.
(2) provide surface abundances of Fe, Si, and K and infer alkali depletion from K abundance; provide abundance limits on H and S at the poles.
(3) map surface element abundances where possible; otherwise provide surface-averaged abundances or establish upper limits.

These objectives are a distillation of the PLR objectives applied only to the GRS portion of the GRNS instrument, and have been refined after a further analysis of specific elements and their abundances needed for determination of planetary evolution.

Because the orbits around Mercury are highly asymmetric, the observation time at low altitudes where elemental gamma-ray fluxes are detectable is quite limited. In order to attain sufficient sensitivity, it is necessary that the GRS detector have the high energy resolution available only from a high-purity Ge crystal. Ge must be cooled to ~ 85K for operation, which requires a mechanical cryocooler and very good thermal isolation in the hot Mercury thermal environment. The Ge is also subject to radiation damage by cosmic rays. To maintain its high resolution, occasional annealing at 80C or more is required, so a zener diode crystal heater circuit is provided. To maintain the high resolution of the Ge detector in flight, a substantially more precise set of ground calibrations is required than for a scintillator based system.

A cut-away view of a CAD model of the GRS sensor is illustrated in Fig. 1. The Ge gamma-ray detector crystal is encapsulated in a nitrogen-pressurized Al cylinder, which is thermally isolated by a Kevlar-string suspension and nested low-emissivity radiation shields. Electrical leads extend from the capsule through feedthroughs to a preamplifier and a high-voltage filter onboard the sensor. The detector is cooled by a small rotary Stirling cryocooler, which has been preselected and customized by the manufacturer to deliver improved performance and extended lifetime. A cooler controller feedback loop monitoring a temperature diode maintains constant detector temperature. All feedthroughs have vacuum seals, so that when a pump hat is screwed onto the top of the sensor, the detector interior can be evacuated. This allows convenient operation of the detector on the ground without a vacuum dewar enclosure, including full operation when the detector is mounted on the spacecraft (allowing complete final checkout prior to launch).

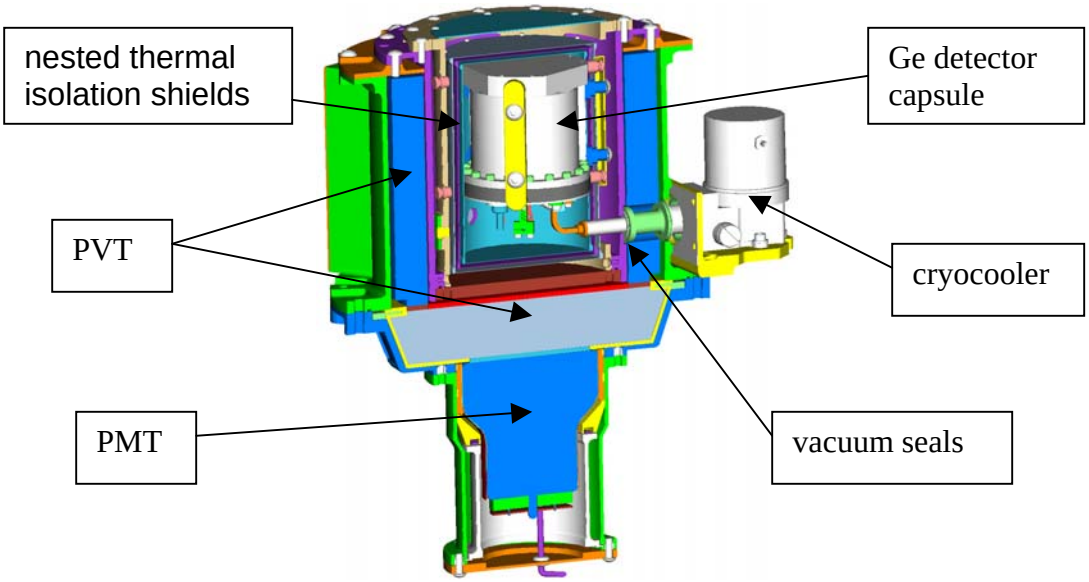


Fig. 1. CAD cutaway illustration of GRS sensor.

Surrounding the detector cage is an annular cylinder of plastic scintillator (PVT, polyvinytoluene) optically coupled to a bottom endcap of plastic scintillator, that is optically coupled to a photomultiplier tube (PMT), which forms an anticoincidence shield. The primary purpose of this shield is reduction of on-scale cosmic ray background in the Ge detector. The PVT contains 5 weight percent natural boron,

which preferentially captures neutrons that thermalize in the plastic, largely preventing them from being captured by H instead, which would lead to a characteristic H gamma-ray that could be absorbed by the Ge detector and appear as a false H signal from Mercury. An anticoincidence mode is also available with the 478-keV gamma-ray emitted by $^{10}$B when it captures a neutron, which yields a neutron flux estimate (for use in background subtraction) and can largely eliminate the $^{10}$B gamma peak in the Ge detector spectrum.

Figure 2 is a photograph of the GRS flight unit on a test stand just prior to installation on the spacecraft, including the sensor and electronics box. Also shown attached to the cryocooler mount and stator is the passive radiator, which always points to cold space, away from the planet and the Sun, to remove heat generated by the cooler and radiated to the sensor by the planet. Visible are the preamplifier and high voltage filter boxes on the outside of the sensor. The electronics box includes electronic and high voltage power supplies for the Ge detector and PVT shield, preamp and amplifier for the PVT shield, Ge shaper amplifier with digital sampling designed to remove cooler vibration contributions to electronic noise, power and controller for the cooler and anneal heater, instrument EPU (Event Processing Unit), and downloaded software.

The MESSENGER Gamma-ray Spectrometer (GRS) produces three gamma-ray spectra during each integration period. When a gamma ray interacts with the detector material, a charge is generated. The amount of charge is proportional to the energy of the photon. The amount of charge is measured and then converted into the appropriate channel number, which is proportional to energy. The three spectra are: (1) all interactions in the primary Ge detector, the raw Ge spectrum; (2) all interactions in the plastic shield, the plastic spectrum; and (3) all interactions in the primary Ge detector that are not in coincidence with an interaction in the plastic shield, the Ge anticoincidence spectrum. The first and third spectra are sorted into 16384 14-bit channels and the second spectrum is sorted into 1024 14-bit channels. Gamma-ray energy deposition as a function of energy (channel number) is recorded over the commanded integration time period.

The ground calibrations were performed on the flight detector system before launch. From experience gained with the Mars Odyssey (MO) GRS and the Near Earth Asteroid Rendezvous (NEAR) XGRS (Goldsten et al, Sp. Sci. Rev. 82, pp 169-216, 1997), it was learned that many of the calibrations can be done separately on components. Some calibrations can be done with the flight electronics and a simulated detector (that acts as a gamma detector front-end), some with the flight detector and laboratory electronics, and some require both the flight detector and the flight electronics (end-to-end tests).

The initial calibration plan draft was generated by Dr. Larry Evans of Goddard Space Flight Center based mostly on the Mars Odyssey GRS calibration test results (2001 Mars Odyssey GRS Calibration Report, October 1, 2001, version 2.0, by Kerry, Marcialis, and Hamara). The MO GRS is a 67 mm X 67 mm high-purity (HP)Ge detector that uses a passive radiative cooler. The MESSENGER GRS is a 50 mm X 50 mm HP Ge detector that has an active mechanical cooler and a borated-plastic anticoincidence shield. Many of the important issues that were addressed in calibration of the MO detector system are similar to those of the MESSENGER GRS detector system, and experience gained from MO was utilized to optimize the MESSENGER calibration. The draft plan was modified and extended by Dr.

Edgar Rhodes and Mr. John Goldsten of JHUAPL and reviewed by the MESSENGER Geochemistry Science Team to yield the final calibration plan.

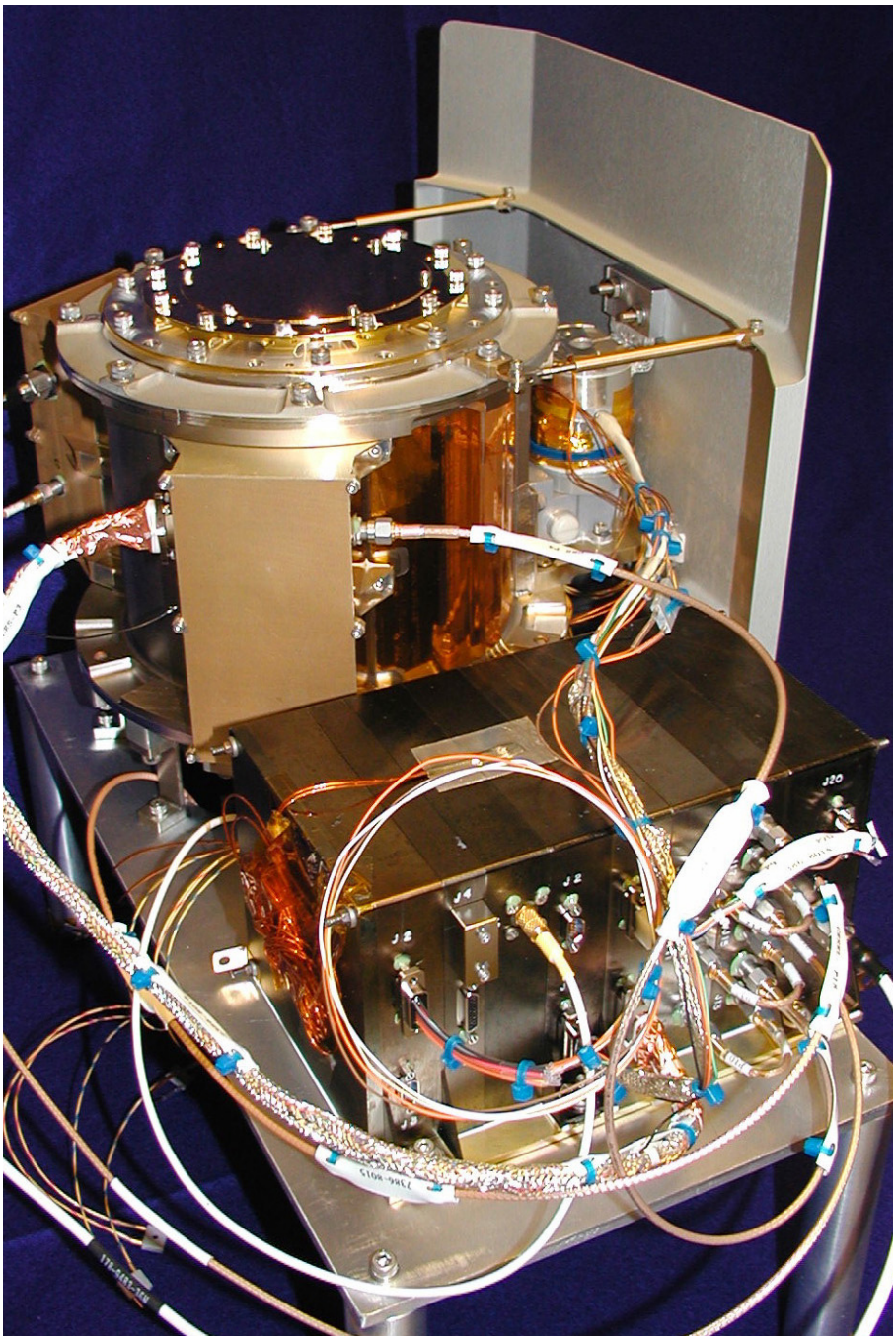

Fig. 2. Photograph of GRS flight unit on test stand.

Most of these calibration measurements require fitting a function to gamma-ray or pulser peaks. The results can be used to determine position and/or peak areas. Both of these quantities can be determined using standard peak fitting routines. One of these codes often used is GANYMED, developed at the

Max-Planck-Institut für Chemie, Mainz, Germany, and used extensively on the Mars Odyssey GRS flight data. There are also IGOR codes that were developed to analyze gamma-ray calibration spectra at the University of Arizona. Many laboratory multi-channel analyzer (MCA) systems have built in analysis programs. For analyzing spectra with large signal-to-noise peaks, whether gamma ray or pulser, most analysis software gives results that are fairly consistent. For MESSENGER GRS calibration bench measurements and tests, Ortec Maestro32 and Aptec MCArd spectral analysis software were used.

Most tests described in the following sections deal with measuring gamma ray spectra. The spectra are usually visualized through a multi-channel analyzer (MCA) or the ground support equipment (GSE) throughout the measurement. Quick look verification can take place by observation of the spectra taken over a short time interval. A quick analysis of the test measurements can often be done directly with the software usually available with an MCA. However tests and calibrations requiring full flight electronics must interface to the GSE. Data processed through the GSE normally does not have this spectral analysis capability. Spectra taken with the GSE normally must be converted to ASCII files or analyzed on a computer that can read the GSE output files. However a version of MCArd.DLL was written that was directly interfaced to the GSE operating system GSEOS, providing the speed, functionality, and precision of laboratory MCA spectral analysis for GSE measurements.

The following tables summarize the calibration measurements, the required components (laboratory or instrument), and the scale of measurements and priority for pre-launch testing. The science team members recommended these priorities to the instrument scientist and instrument engineer. The spatial calibration takes the most time, but is also one of the highest priority measurements. Time required for spatial calibration depends on spatial resolution of the measurements. To fit measurements into time available, the strategy is to start with coarse spatial measurements centered around the on-axis direction and fill in with finer spatial resolution measurements as time allows. There will be an absolute minimum number of off-axis points; for example, 12 points determined for optimal sampling of the angular response. In addition, engineering drawings indicate specific angles of maximum gamma attenuation that should be sampled.

A significant factor that must be considered by the instrument engineer and instrument scientist in optimizing measurement time required for the overall suite of calibration measurements requiring operation of the GRS sensor is the limited lifetime of the GRS cyrocooler, which is expected to be not much longer than the one-Earth-year orbital mission. Once the 200-hour infant mortality operational time is exceeded, any operation of the cooler can be viewed as taking lifetime away from the orbital mission. Since ~ 1.5 days is required to cool down the Ge detector to operating temperature, operational time is optimized by making as many measurements as possible during every operational period and by minimizing total measurement time requiring sensor operation.

Tables I and II below provide the geochemistry science team recommended calibration measurements, along with priority and estimated duration.

Table I. Recommended Measurements

| Measurement | Components |
|---|---|
| **DNL** | **Electronics-detector simulator** |
| INL | Electronics-detector simulator |
| Gain/Offset | Detector, Flight |
| Internal Pulser | Electronics |
| Resolution, Muon | GSH, Electronics (pre-amp/shaper only) |
| Resolution, ETE | GSH, Electronics |
| LLD calibration | Electronics-detector simulator |
| Spatial calibration | GSH, laboratory electronics |

"GSH" is defined as the gamma-ray sensor head.

Table II. Priority & Estimated Duration of Measurements

| Measurement | Priority | Test Duration |
|---|---|---|
| DNL | 1 | 3-5 days |
| INL | 1 | 1 day |
| Gain/Offset | 1 | 7 days |
| Internal Pulser | 2 | 1 day |
| Resolution Muon | 3 | 1 day |
| Resolution: ETE | 2 | 5 days |
| LLD | 3 | 1 day |
| Spatial calibration | 1 | 1-3 weeks |

Where the priorities are: 1 – required, 2 – desirable, and 3 – if schedule allows.

A calibration measurement not mentioned in the above tables is gain vs. high voltage for the GRS anticoincidence shield. This measurement was performed during the final CPT test at Astrotech.

**Summary of As-built GRS Specifications**

Below is a table summarizing fundamental specifications for mass, dimensions, power, etc. and various important calibration values for the mission for the GRS instrument in its as-built configuration.

Table III. GRS Specifications & Calibration Summary

Total mass: 9.43 kg

Maximum operational power: 23 W

Maximum survival power: 16.5 W

Maximum data rate: ~5000 signal events per second

Differential nonlinearity: < count statistics (unmeasurable)

Intergral nonlinearity: < 2 channels out of ~15,000

Electronics box temperature offset: < 0,2 channels

Electronics box temperature gain drift: < 20 ppm/C

Preamp temperature gain drift: < 95 ppm/C

Pulsar temperature gain drift: < 50 ppm/C

Energy resolution FWHM, keV: 3.34 @ 121, 3.49 @ 1332, 44.77 @ 6130

Pulsar resolution FWHM, keV: 3.07 @ 7985

Intrinsic efficiency @ keV: ~0.236 @ 511, ~0.104 @ 1332, ~0.018 @ 6130

**DIFFERENTIAL NONLINEARITY**

The differential nonlinearity (DNL) of a system is the differences in channel width across the spectrum. This is measured using an input of pulses uniformly over the spectrum for a time sufficiently long so that the statistical fluctuations in each channel are small compared to the measurement accuracy.

**Test Description**
A pulse generator externally triggered by a ramp generator was fed into the flight electronics and gamma simulator. The pulser was operated at a high rate (~5KHz) to accumulate counts quickly, but, as a result, introduced some minor non-linearities. The test was allowed to run for several days to build up ~120,000 counts in each channel, a value consistent with measuring DNL to better than 1%.

**Analysis**
In order to determine a measure of the total DNL and values for the individual periodicities of an arbitary DNL data set, generally the data must be processed to remove systematic spectral trends by

fitting to a polynomial. In addition to the total DNL, individual periodicities among the channels also usually need to be investigated. However the flight analog-to-digital converter (ADC) has a dither circuit, so there should be no set DNL patterns. A low-order fit was used to remove the non-linearities of the pulser system and the residual is shown in Fig.3. The dither action reduces slightly the overall dynamic range of the system, reducing the number of available channels from 16384 to 15000. It can be seen that the DNL is very low and that there is no overall trend or significant periodicity effects.

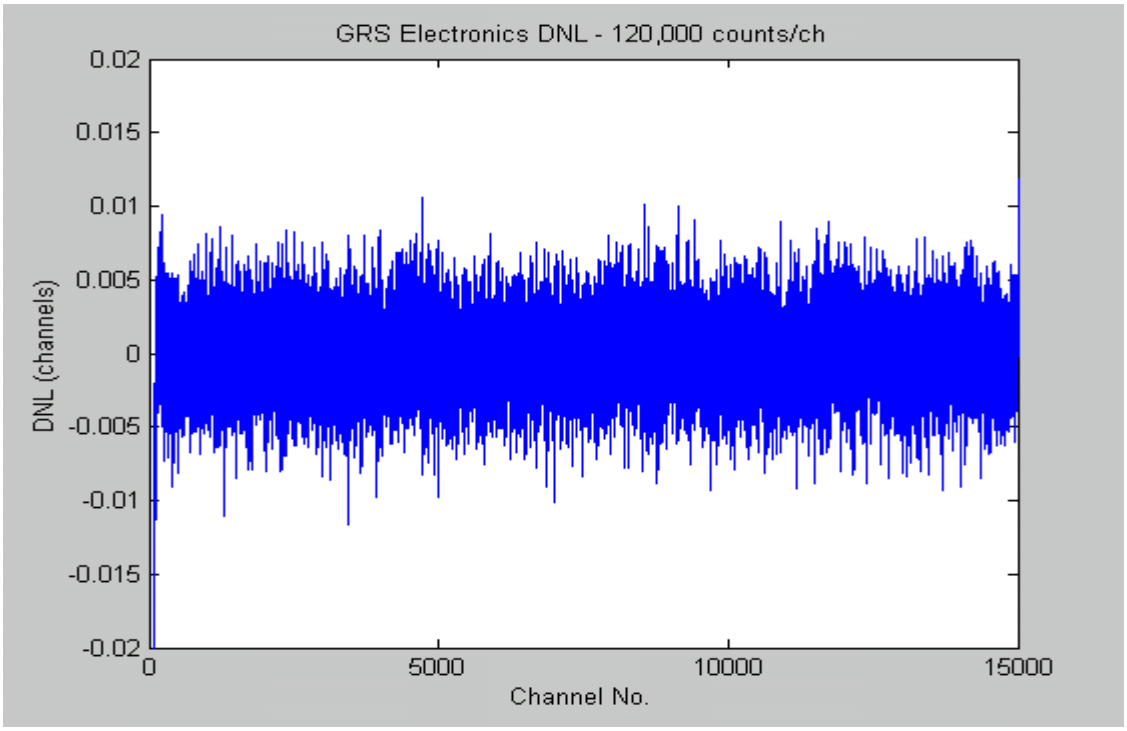


Fig. 3. GRS electronics DNL channel sweeps

The total DNL is calculated first by taking the square of the difference between the counts in each channel in the adjusted spectrum and the overall average counts per channel. These values are then summed together and divided by the total number of channels less 1. The square root of that value is then divided by the overall average counts per channel; this yields a measure of the total differential non-linearity. The sigma value associated with the total DNL is calculated by taking the square root of the average of all counts per channel and dividing by the average of all counts per channel. The goal for the total 3-sigma DNL calculated for the data should be less than 1%. The resulting DNL distribution function in shown in Fig. 4 in counts per 100 channels. With a standard deviation of 0.0027, the 3-sigma value is 0.0081, less than the 1% goal. This is also less than the Poisson standard deviation for 120,000 counts for one channel, which is 0.00289, so the DNL is smaller than count statistics and thus is negligible.

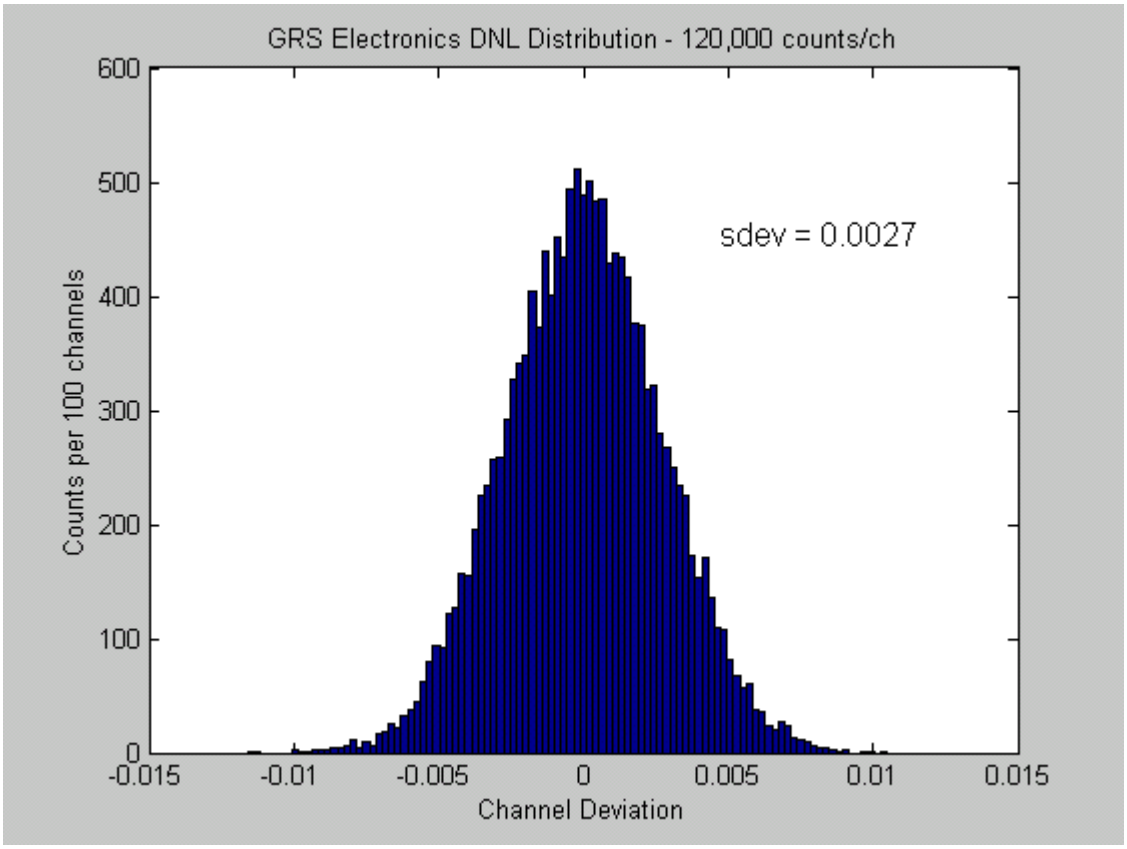

Fig. 4. GRS electronics DNL distribution.

## INTEGRAL NONLINEARITY

The integral non-linearity (INL) of a system is the deviation from an assumed linear fit between energy and channel number measurements when using radioisotope sources or between the calculated and measured channel positions when using a pulse generator.

### Test Description

During this test the flight electronics (not including the preamp) was in a climate chamber. A precision pulser was used to characterize the INL by manually adjusting its precision attenuator to approximately 50 different equally-spaced settings. For each setting, 500 pulse height samples were captured and averaged to reduce noise. The pulser rate was kept low (~50Hz) to maintain linearity. The chamber was set to four different temperatures over the temperature extremes predicted to occur for the GRS electronics box, with added temperature to compensate for the lack of a vacuum, or from -30°C to 64°C.

### Analysis

Data plotted in Fig. 5 shows the residual INL after subtraction of a simple linear fit. The INL spread over the spectrum is largest at -30°C, 2.5 channels, and smallest at 64°C, 0.8 channels. The dip in the middle of the spectrum seen in Fig. 5 is probably the result of fitting to an overall sublinear INL in the

laboratory measurement system. (It is difficult to find commercial components with very low INL). The maximum INL spread is thus probably less than shown in Fig. 5, closer to 1.5 channels.

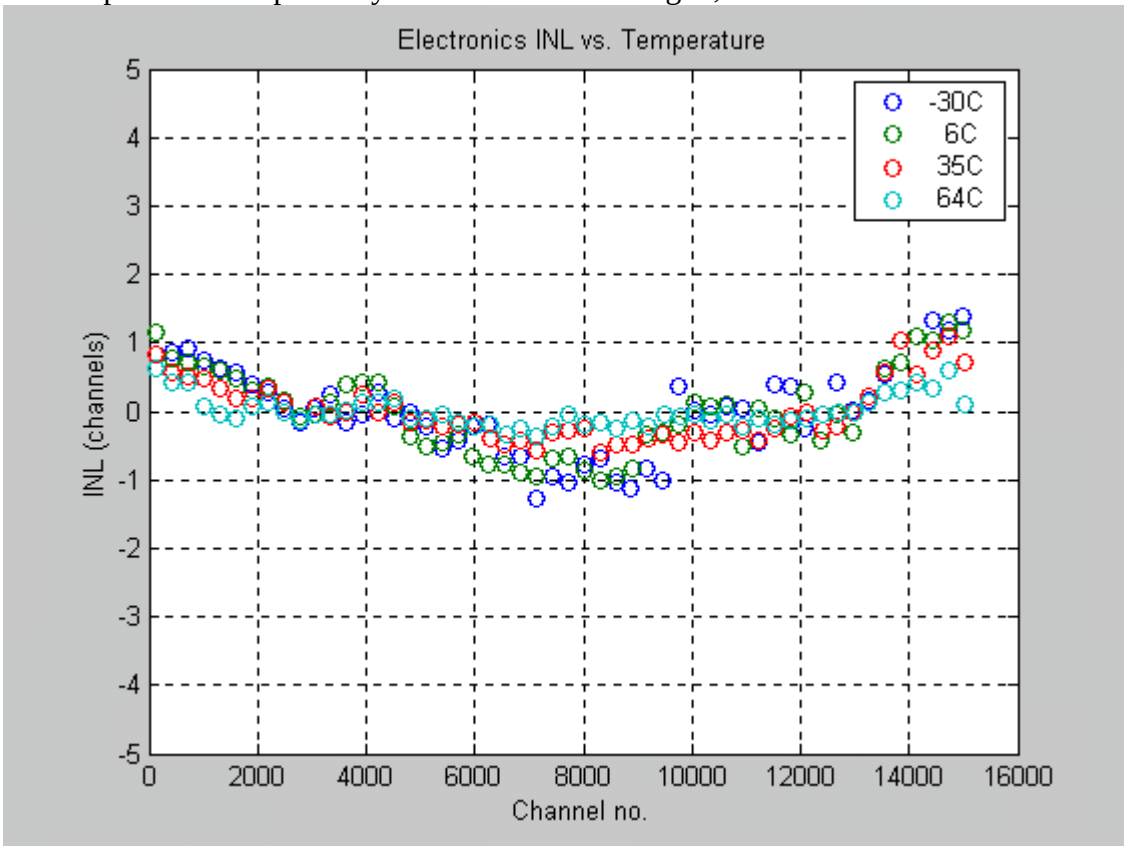


Fig. 5. GRS electronics INL at various temperatures.

The Ge energy scale is 0.605 keV/channel, so the $^{60}$Co 1332 keV line is at channel 1997. In Fig. 5, the INL change in that channel region over the full temperature range is ~ 0.4 channel. With an energy resolution of ~ 3.4 keV, the full peak covers ~ 17 channels, and 0.4 channels is only 2.4% of 17 channels, not a problem. The largest full temperature INL changes are 1.2 channels at ~ channel 15,000 and 1.0 channels at ~ channel 7200, but the energy peaks cover substantially more channels at these points. The biggest concern is temperature changes over an orbit, especially the spike when low altitude is reached, but the temperature of the electronics box should not change much in this case, since the box is thermally coupled to the deck. INL correction does not appear to be necessary.

## GAIN AND OFFSET

The gain and offset of a system gives the energy-channel relation as a function of other variables, such as temperature or voltage settings. The gain is the energy per channel and the offset is the energy at channel zero.

### Test Description

The temperatures of the individual components of the detector system will affect the signal pulse height and thus have an impact on the measured gamma spectra. Each of these components displays a unique behavior in response to a change in temperature. In each case, this behavior can be characterized in

terms of a gain and an offset with respect to the gamma spectra. For each component, then, a correction based on temperature is derived, such that the collected gamma data can be adjusted accordingly.

Comprehensive end-to-end data was taken during the instrument TV test using a $^{60}Co$ radioisotope source. The bulk temperature of the GRS Sensor and the GRS Electronics were varied independently. That data, which is expected to be very similar to those tests described below done with pulsers, will include any subtle effects due to thermal gradients. This test data has not yet been analyzed. The GRS contains internal temperature sensors at each stage of the signal processing chain and all of these temperatures are available on-orbit if such second-order corrections become necessary.

Gain characteristic measurements were also made using a thermal climate chamber and an external pulser. The GRS Preamp and the GRS Electronics were measured separately. The GRS Electronics measurement includes contributions from the shaper, programmable gain stage, ADC, and voltage reference, as well as any parametric influences due to the temperature dependence of the power supplies. Measurements were made at discrete temperature plateaus and during temperature ramping.

**Analysis**

Shown in Figs. 6 and 7 are the electronics gain drift and offset vs. temperature for the pulser tests in the climate chamber. Gain drift is 20 ppm/°C or less and thus will not have much effect on the energy calibration (one channel represents 60ppm of full scale). The offset shows negligible dependence on temperature, being held to within 0.5 channels over the full 100 °C temperature range. This is a result of the design of the pulse processing system, which captures both the positive and negative peaks of a bipolar pulse and digitally computes the difference. This technique effectively “auto zeroes” the system on a pulse-by-pulse basis, and eliminates those offsets due to pole-zero mismatch, dithering, and even those offsets generated within the ADC itself. The data clearly shows the efficacy of this approach.

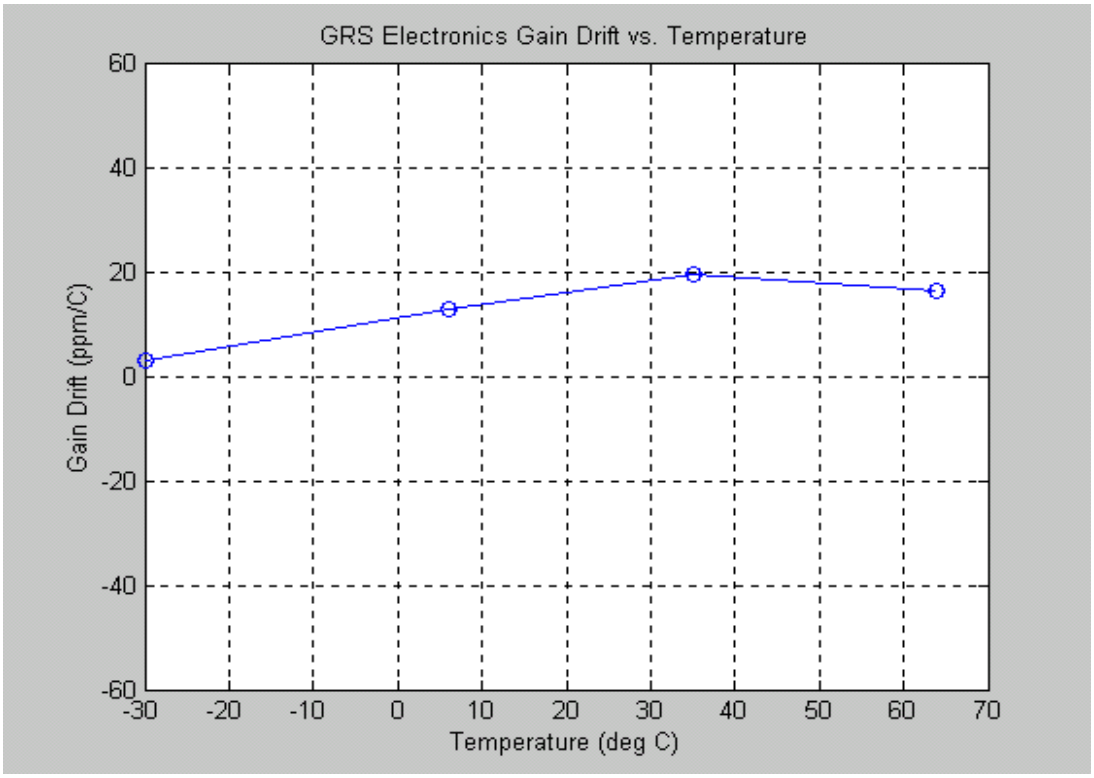


Fig. 6. Gain Drift with temperature for electronics box.

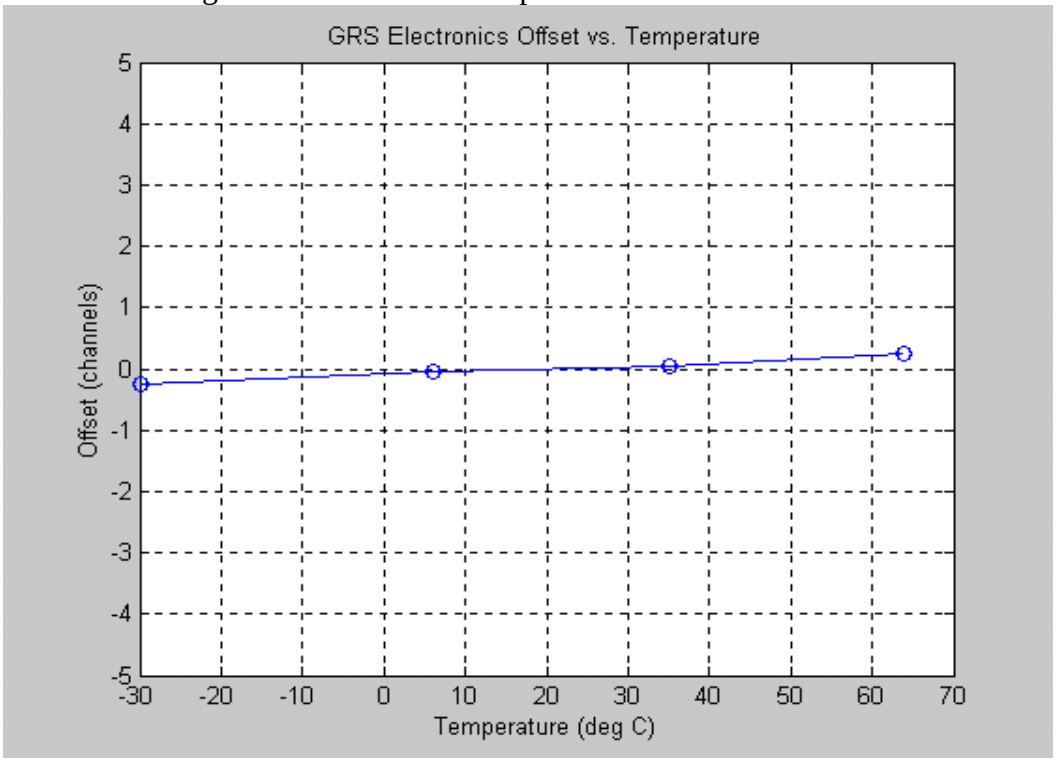


Fig. 7. Offset vs. temperature for electronics box.

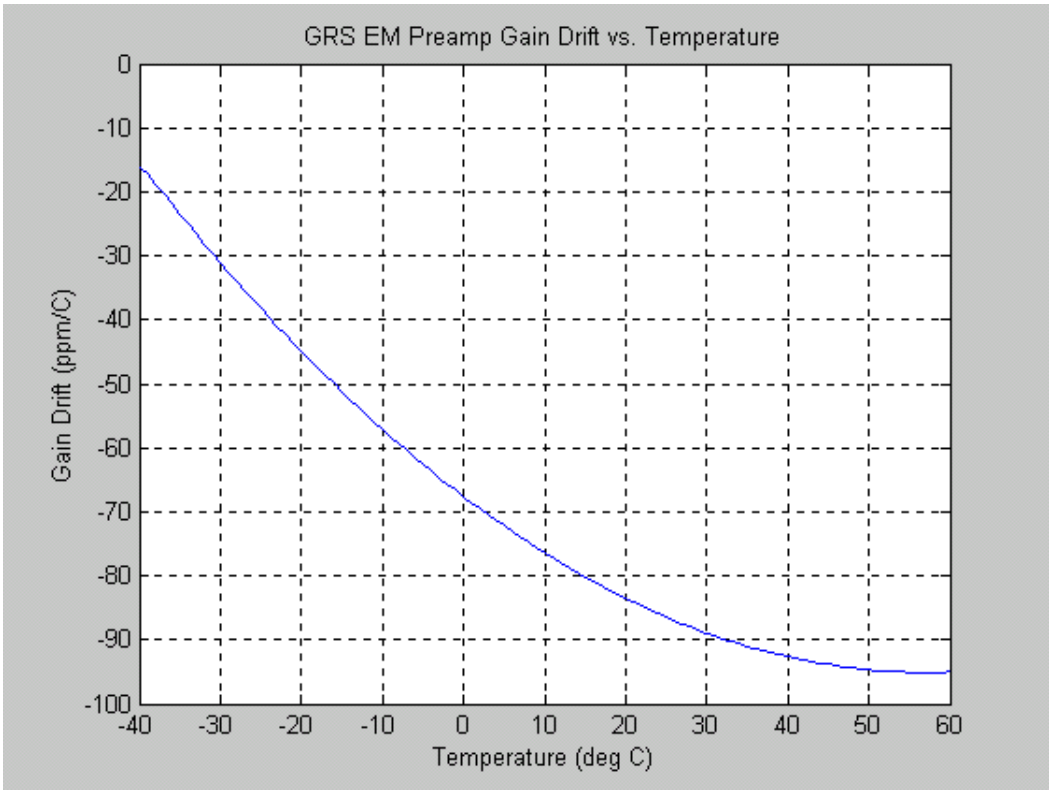

Fig. 8. Preamp gain drift with temperature.

As can be seen in Fig. 8, the gain characteristic of the GRS Preamp shows a more dominant dependence on temperature and reaches nearly 100 ppm/C under hot conditions. Thus small corrections for the GRS Preamp temperature will likely be required. Fortunately, because offset is not a problem, only gain corrections will be necessary, thus simplifying the correction.

## INTERNAL PULSER

The purpose of the internal pulser is to provide an internal reference for gamma data collected during flight. Calibration of the internal pulser is required to understand how the position of the reference changes with external factors.

### Test Description

There is one internal pulser built into the gamma system at a specific energy slightly less than 8 MeV. Because the internal pulser is energy specific, its position changes with varying shaping amplifier gain. But also, the internal pulser is comprised of electronic components that reside in both the GRS Sensor and in the GRS Electronics (as well as the cable between them). Therefore, each contribution must be separately characterized. Comparison with a reference energy line from a radioactive source was judged to provide the best and most accurate source for this type of calibration. End-to-end data was taken during instrument TV tests using a $^{60}$Co radioisotope source. The bulk temperature of the GRS Sensor and the GRS Electronics were independently varied.

**Analysis**
Preliminary analysis of a few data points suggests that the internal pulser correctly tracks variations in the sensor preamp, and that its own temperature coefficient (sensor component only) is at least a factor of two lower than the preamp. Pulser variations due to temperature changes of the components inside the GRS Electronics have yet to be analyzed, but in general should be less critical as the GRS Electronics does not experience the dramatic temperature swings the sensor sees as it traverses the hot planet. Noise width of the internal pulser line consistently measures 3.0 keV FWHM, which provides a good diagnostic of the state of the preamp, especially for cases in which the energy resolution of the detector has degraded due to radiation damage.

## ENERGY RESOLUTION

Energy resolution is the width of the gamma-ray spectral lines and will vary with gamma-ray energy, usually specified as full-width at half-maximum (FWHM). It is the most important specification for the Gamma Ray Spectrometer. It determines sensitivity (i.e. signal-to-noise ratio) and the ability to resolve closely spaced peaks.

**Test Description**
Energy resolution is the only parameter called out at the subsystem level. The gamma sensor head has its own specification (4 keV goal for 1332 keV) that can be demonstrated with conventional laboratory electronics or flight electronics.

Testing for the space cosmic ray overload effect on energy resolution is difficult because there are no cosmic rays on the surface of the Earth. Muons can be used as an analog for cosmic rays. Muons are a by-product of cosmic-ray interactions in Earth's atmosphere. They are a good analog to cosmic-ray protons in terms of energy deposited, though they do not duplicate the cosmic-ray alpha particles, which deposit much more energy. The cosmic-ray count rate in space is estimated at about 200 Hz (from another flight GRS), but is much smaller on the ground. During muon resolution testing, radioisotope sources are counted, but only events which occur in less than or equal to 5 msec (5 msec = 200 Hz) after a muon event (i.e. events greater than 8 MeV) are accepted for analysis. Unfortunately the muon test is incompatible with the GRS electronics. The unique pulse-processing methods employed in the GRS cannot be accurately duplicated using standard laboratory electronics and the GRS is not designed to accept an external hardware gating signal. At one time, a software solution was discussed, but was overtaken by events of higher priority. The muon test may not be very effective anyway. For Mars Odyssey it gave identical energy resolution to that measured with radioisotope sources normally.

However, the GRS signal processing chain contains several features that mitigate any possible effects due to cosmic ray overloads. First, the charge-sensitive preamp has charge-reset capability to recover quickly (~10us) from overloads greater than 100 MeV. Under the same conditions, a standard preamp might remain in a saturated condition for several milliseconds. Not only does such a condition introduce additional dead time, but while the preamp is saturated, a serious pole-zero mismatch develops resulting in baseline errors that can accumulate and take time to settle. With charge-reset active, the GRS recovers from most overloads in nearly the same amount of time as for in-range pulses. Even with charge-reset disabled (a commandable feature), the "tri-polar" shaping technique employed in the GRS

dynamically eliminates baseline errors due to pole-zero mismatch. These features were tested using a high-level square-wave pulser capable of simulating >1 GeV pulses.

Most cosmic rays (perhaps 90%) will likely deposit less than 60 MeV in the detector and will therefore stay within the linear range of the preamp. The shaper networks will of course saturate, as they are designed for 10 MeV full scale, but they recover relatively quickly and the tri-polar shaping technique reduces any residual errors. Pile-up rejection circuitry further mitigates the effects of overloads and the settling window for events is set within the FPGA and is commandable in 1μs increments. Optimized values were determined using an overload pulser.

The MESSENGER GRS has an additional source of noise from the mechanical cooler that may contribute to the energy resolution. A series of energy resolution measurements was made using $^{60}$Co with both the cooler running and with the cooler temporarily off. When the cooler was turned off, the detector temperature would rise quickly enough that integration times were limited to 120 sec to limit energy smearing. There was no significant difference in energy resolution with cooler on vs. cooler off. This result suggests that either the microphonics generated by the cooler are sufficiently isolated as to not adversely affect the preamp, or that the GRS tri-polar shaping technique is so unsusceptible to the effects of microphonics that one doesn't see a difference, or a combination of both. This question can only be answered by taking additional measurements with standard laboratory electronics to characterize the effects of microphonics for different pulse shapes (unipolar and bipolar) and as a function of shaping time. No further tests in which the cooler is turned on and off were conducted on the flight detector, because it was noted that turning the cooler off while high voltage is still applied to the detector may lead to a coronal discharge due to deposits boiling off the cold finger.

**End-To-End (ETE) Resolution.** The best simulation of the flight-like conditions for temperatures and operating with other instruments is with the detector mounted on the spacecraft during thermal-vacuum (TV) tests. Data from these tests have not yet been analyzed, but will be analyzed before needed for instrument operation in space. Using radioisotope sources, a room-temperature CPT of the end-to-end flight unit on the spacecraft with all other instruments operating has been conducted and analyzed, using Aptec MCArd software to determine FWHMs. The results are shown in Table I. No escape peaks are included. In order to conserve cooler lifetime, the tests have limited measurement times and thus limited counts accumulated in some peaks, particularly at high energy. Accumulated counts (minus background) are given in the table, to indicate which peaks have FWHMs with more measurement uncertainty.

Table I. ETE Energy Resolution Measurements

| Energy, keV | FWHM, keV | Counts in peak | Source |
|---|---|---|---|
| 7985 | 3.07 | 26721 | pulser |
| 6130 | 4.77 | 974 | PuC-13 |
| 3548 | 3.97 | 217 | Co-56 |
| 3451 | 4.24 | 978 | Co-56 |
| 3273 | 4.37 | 2060 | Co-56 |
| 3253 | 4.44 | 9213 | Co-56 |
| 3202 | 4.07 | 3679 | Co-56 |
| 3010 | 3.66 | 1166 | Co-56 |
| 2598 | 4.05 | 24191 | Co-56 |
| 2035 | 3.77 | 13961 | Co-56 |
| 2015 | 3.64 | 5422 | Co-56 |
| 1771 | 3.73 | 31130 | Co-56 |
| 1360 | 3.53 | 10214 | Co-56 |
| 1332 | 3.49 | 130741 | Co-60 |
| 1238 | 3.59 | 170942 | Co-56 |
| 1173 | 3.44 | 140235 | Co-60 |
| 1038 | 3.48 | 39016 | Co-56 |
| 847 | 3.47 | 319479 | Co-56 |
| 121 | 3.34 | 24037 | background |

**Analysis**

The pulser peak in Table I of course is not indicative of ETE resolution. The radioisotope source gamma peaks shown span nearly all gamma-ray energies of interest. It is seen that the energy resolution goal of 4 keV at 1332 KeV is exceeded by 0.5 keV. In fact, peaks of energies exceeding 3000 keV have resolutions ~ 4 keV. Resolutions at low energies approach 3.3 keV and are limited primarily by noise, probably from the cryocooler. The resolution of ~ 4.8 keV at 6130 keV is very good.

## LOW LEVEL DISCRIMINATOR FUNCTIONALITY

The low level discriminator acts as variable, virtual barrier within the digitized gamma spectra. It is used to exclude electronic noise at the low end of the spectral range.

**Test Description**

Tests need to be performed in order to characterize the functionality and behavior of the lower-level discriminator (LLD) for each detector. The discriminator has a digital value that can be set from 0 to 16384. Those settings correspond to real positions in gamma spectrum channels. A scalar value for the number of counts associated with each discriminator is reported with each gamma spectrum. The LLD scalar returns the number of counts in spectrum that are above the LLD barrier (events below the LLD level are not processed). The LLD settings have been calibrated with respect to channel positions.

**Analysis**

The GRS pulse processor does not contain an analog comparator, but rather implements level discrimination inside the FPGA based on the difference of successive ADC samples. As a result, the LLD function is exceedingly stable and does not exhibit problems normally associated with analog components, such as sensitivities to dc offset, crosstalk, hysteresis, etc. The GRS LLD currently is set to ~ 60 keV, which is above the noise level but well below the 300 keV signal requirement. Such margin

makes detailed characterization of the LLD less important. However, a series of LLD tests were performed during the final GRS CPT to determine the LLD conversion factor more precisely and any effects on system throughput.

## GRS SPATIAL CALIBRATION

The purpose of the spatial calibration is to map out the spatial (angular) response of the GRS sensor head to photons incident on the detector from a distance that is large compared to the detector dimensions, at all energies and angles of interest for detection and mapping of elements of Mercury's crust. This amounts to determination of the effective area or intrinsic efficiency of the GRS over a wide range of energies and angles, corrected for energy and angle dependent attenuation of the radioisotope sources in the experimental setup and associated with the position of the GRS on the spacecraft. A sufficient number of counts must be accumulated for each energy peak at each angle to yield count statistics that will allow an accurate assay of elements composing the crust.

### Test Description

This is the most time consuming and complex portion of the calibration. Measurements taken at Mercury must be converted from counts in the detector to photon flux incident on the detector. There are several complicating factors other than the geometry of the crystal which must be taken into account. For example, blocking due to instrument and spacecraft structural members will modify an otherwise smoothly varying response function. How much these structures attenuate a gamma- ray source is itself a function of the geometry and composition of the structural member: each material has its own unique properties. Both the intrinsic detector angular response and "shadowing" by structural members are functions of the energy at which the photon response is being measured.

The GRS is located on the spacecraft close to the Al adapter ring, which presents a particular external structural member that attenuates the spatial response to the planet, so its effect must be determined either experimentally and/or computationally. There is only one ring and it was mounted on the spacecraft at the time the spatial calibration was needed. Spacecraft testing requirements did not permit GRS calibration measurements with the GRS mounted on the spacecraft. The instrument scientist estimated the total viewfield attenuation of the ring was only ~ 7% at 440 keV (main Na neutron inelastic scattering gamma) and ~ 2% at 7646 keV (main Fe neutron capture gamma doublet). With concurrence of the Geochemistry Science Team, the instrument scientist determined that the ring attenuation angular dependence can be satisfactorially calculated using exponential attenuation with the aid of a CAD program to determine thicknesses of the ring rib structure. This fairly tedious computation has not yet been done.

In practice, the response of GRS will be a convolution of these effects with the "point source" measurements of the calibrations. To maximize mapping resolution, a scheme to deconvolve these effects to some approximate level needs to be devised. The Gamma Sensor Head detects gamma rays from all directions ($4\pi$sr). For mapping in orbit around Mercury, the GRS has an effective field-of-view defined by the solid angle subtended by Mercury, which will change as a function of time throughout each orbit due to spacecraft altitude changes. Centered on the nadir direction, this angle is described by a half-cone angle given by $\Theta = \sin^{-1} [1+h/R)]^{-1}$, where R is the radius of Mercury (2440 km) and h is the spacecraft altitude, assuming the planet is spherical.

The orbits will be highly asymmetric, with the closest distance ~ 200 km defining the largest cone (and the most sensitive measurements, having the highest gamma flux). By this formula, sensor-head response to the planet is limited to a half-cone angle of 67.55°. It is strongly desirable to make measurements at a lesser number of angles over the full unit sphere, in order help determine and correct for background and for non-nadir pointing measurements. However, it was the judgment of the instrument scientist to constrain the spatial calibration of the flight unit to 37 fairly equally spaced angles in the forward 67.55° cone only, in order to conserve cryocooler lifetime, in view of the limited mapping resolution that can be attained for the small time spent in orbit at low altitudes. The flight spare unit is available for further calibration measurements (but it has no lower housing to represent true gamma attenuation and scattering properties at large angles). The Geochemistry Science Team concurred with this limit.

The gamma-rays of interest extend from the Na inelastic scattering line at 440 keV to at least the 7646 keV Fe capture doublet, and measurements at lower and higher energies are desirable to improve efficiency accuracy near the ends of the spectrum. Previous spatial calibrations of Ge space-flight gamma-ray spectrometers have relied on radioisotope sources, which are available with reasonably high source strengths, reasonably long half-lives, and reasonably accurate calibrations with gamma-rays only up to ~ 3500 keV, with weak approximately calibrated sources at 6143 keV. Efficiencies at higher gamma-ray energies were generally extrapolated using Monte Carlo computations and were not well characterized.

The instrument scientist decided to conduct the spatial calibration of the GRS flight unit at the National Institute of Standards & Technology reactor, where intense beams of cold neutrons are available to irradiate neutron-capture targets and excite strong fluxes of gamma-rays across the entire energy range of interest. This allowed sufficient data rates at high gamma energies to complete the calibration in only 5.5 days of 24-hour measurements, which minimizes impact on cooler lifetime while providing superior efficiency accuracy across the desired energy range. Targets of Cr and Cl were chosen, which provide many strong gamma peaks in the range from 517 to 9717 keV, with intensities well characterized by recent International Atomic Energy Agency standards. These targets provide only relative efficiencies, because the neutron fluxes and cross-sections are not known accurately enough to yield absolute efficiencies. To normalize efficiencies to be absolute, fairly strong sources of $^{56}$Co (100 μCi), $^{226}$Ra (10 μCi), and $^{228}$Th (10 μCi) were procured and calibrated by NIST. These sources provide many strong gamma peaks between 239 and 3451 keV and complement the capture target peaks by having more lower energies but many peaks in the same range as the capture targets, to get proper normalization.

**Configuration.** The signal from the GSH preamp was fed into both a laboratory digital signal processor unit (Ortec DSPEC) and the flight electronics box, which controlled the detector and cooler and provided high voltage. The flight electronics signal output was processed through GSEOS. The flight electronics is designed for low signal rates. The DSPEC is designed to process high count rates from Ge detectors while maintaining energy resolution; its signal output was processed through Ortec Maestro32 software, which provided the primary spectra used for the spatial calibration. Preliminary laboratory and NIST tests were conducted using a commercial laboratory Ge crystal somewhat larger than the flight crystal with the DSPEC at high count rates, to check that no significant gamma peak distortions, peak area changes, or energy shifts occurred up to the maximum 30% deadtime encountered during the NIST calibration.

A telescope forked equatorial mount was adapted to hold the GSH and rotate it about the center point of the Ge crystal. A keypad was programmed to rotate the GSH from nadir position (along its cylindrical axis) to 6 equally spaced azimuthal angles at 22.5° from nadir, 12 equally spaced angles at 45° from nadir, and 18 equally spaced angles at 67.55° from nadir, a total of 37 evenly spaced angular positions. A Pb brick shield was set up around the neutron beam of NCNR port NG0 with a hole at right angles to the beam for gamma-rays from a target inserted at 45° to the beam to impinge on the Ge crystal. This shield removes scattered gamma background from the sensor. The Pb brick shield and telescope mount were aligned with the beam on hydraulic lifts such that the distance from the center of the target to the center of the Ge crystal was 47.7 cm.

A view from the back of the GSH in nadir position is shown in Fig. 9. The adapter collar attaching the GSH to the fork mount can be seen. The Ge crystal axis is pointed at the hole in the Pb brick shield viewing the target, which is irradiated by the neutron beam. The beam-target-hole geometry is seen in Fig. 10, which looks down on the Pb brick shield. In Fig. 10, the GSH is pointed at a particular azimuthal angle and 67.55° away from nadir. In Fig. 11, the Si mirror and alignment target frame are used to position the targets and sources and GSH with respect to the beam laser. The NaCl and Cr targets shown are positioned in a target frame that is inserted in the target frame groove shown in Fig. 12. The source holder is positioned over the center of the target frame groove, as shown in Fig. 12, with the three radioisotope sources sandwiched as shown for simultaneous measurement.

A second GSH azimuthal position 67.55° away from nadir is illustrated in Fig. 13. The pump hat and pipe elbow on the vacuum hose block the Ge crystal view of the target. Also in Fig. 10, the edge of the fork mount below the axial hub (not seen) blocks the Ge crystal view of the target. Since these items are not part of the flight unit, their attenuation effects must be corrected for. Similar attenuations requiring correction are present for all azimuthal angles 67.55° away from nadir. The attenuation effects may be estimated analytically or experimentally.

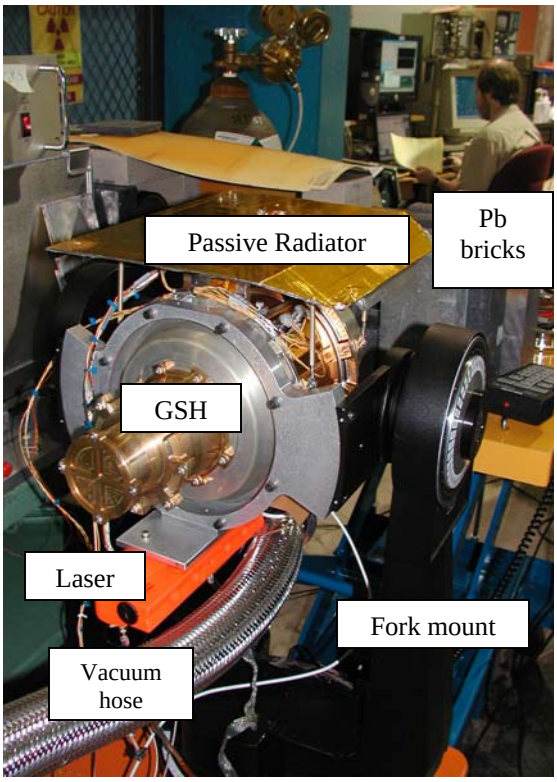


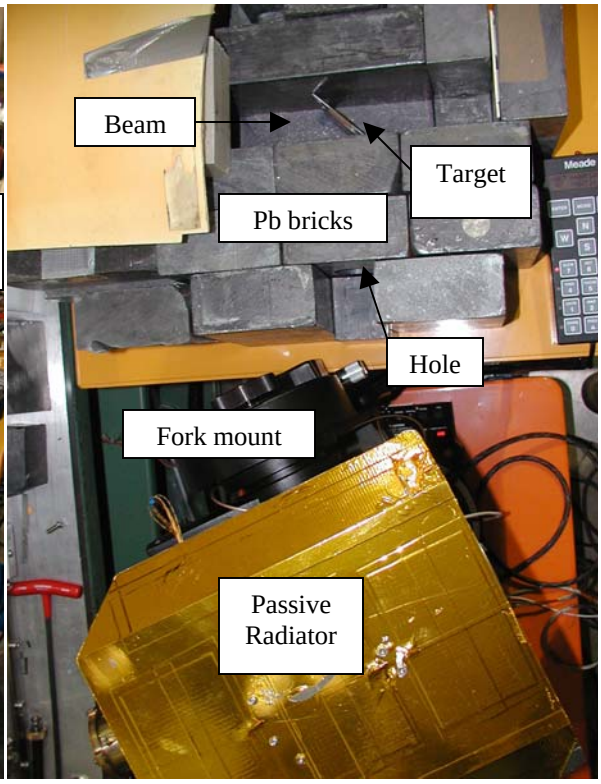


**Fig. 9. GSH at nadir position at NIST NCNR.** **Fig. 10. GSH at a position 67.55° from nadir.**

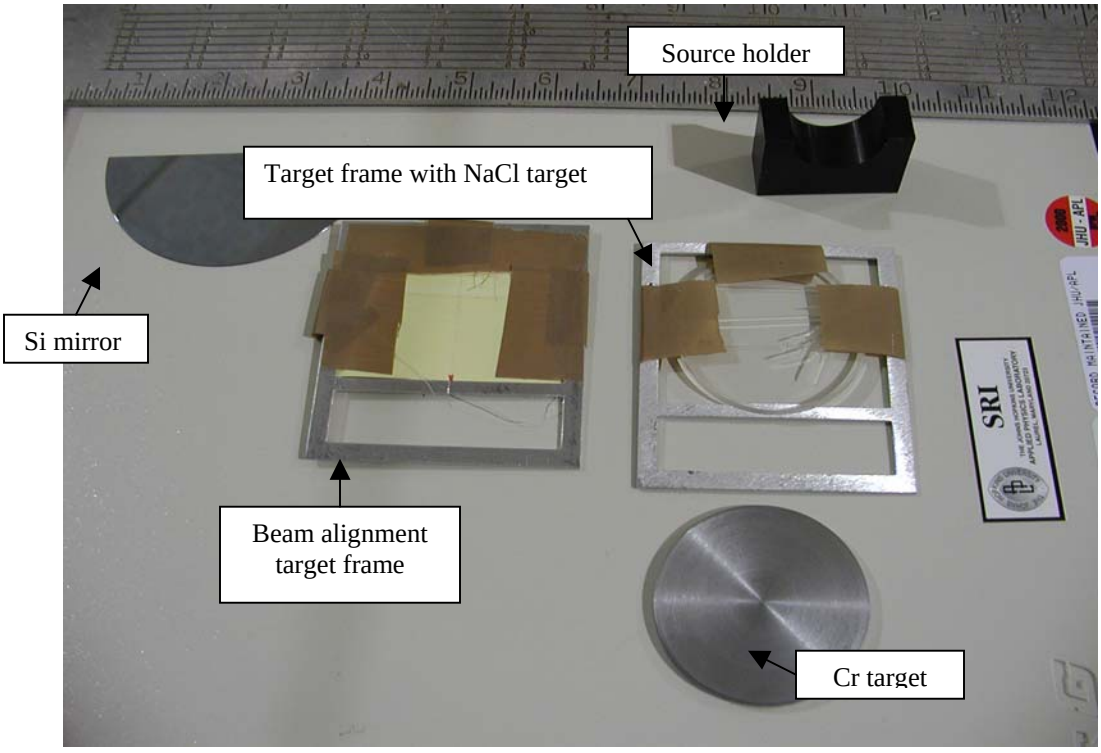


Fig. 11. Items used in NIST NCNR calibration of MESSENGER GRS.

| FSCM NO. | SIZE | DRAWING NO. | REV. |
|---|---|---|---|
| 88898 | A | 7384-9466 | A |
| SCALE | DO NOT SCALE PRINT | SHEET 22 of 34 | |

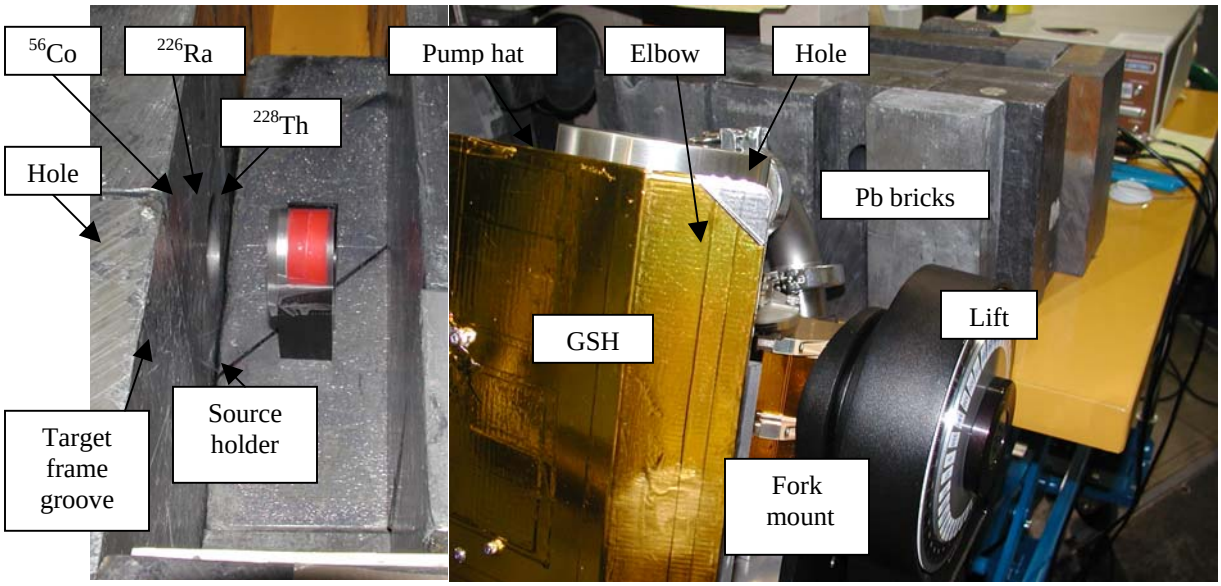


Fig. 12. Source calibration.




Fig. 13. GSH at another position 67.55° from nadir.

Since the pump hat (50 mils thick 6061 Al) covers the front of the GSH, its attenuation is present at all angles. For the nadir direction, the attenuation is easily corrected analytically. The passive radiator is part of the flight GSH, so its attenuation effect does not need to be corrected. Energy-dependent self-absorption/distance corrections for the radioisotope sources and neutron capture targets are the same for all GSH orientations and can be easily calculated.

**Data Analysis**

Data reduction and analysis are being performed using the HypermetPC program, which corrects for INL, fits data peaks, matches them to energies and intensities in a library of nuclides and source strengths, and determines absolute efficiency as a function of energy. Half-lives, dead-times, and estimated data and library statistical errors are accounted for. The library was updated with the latest IAEA standards. Efficiency ε is calculated by fitting lnε to a polynomial in lnE, where E is energy. The polynomial is orthogonal in the matrix subspace related to capture peaks, which improves solution stability. HypermetPC performed well in the latest IAEA standards comparison.

Peak fitting in HypermetPC is performed similarly to the well-known and accepted Hypermet code, with a few more options. For the MESSENGER GRS data, HypermetPC was compared to GANYMED in peak fitting. When both programs fitted strong peaks well, the peak areas (counts) agreed to within 0.1% to 0.4%. HypermetPC was found to fit weak, distorted, and overlapping peaks somewhat better than GANYMED. GANYMED does not have the capability to calculate efficiency.

At the present time, efficiency has been calculated only for the GSH nadir orientation for the DSPEC data, not including escape peaks, but this is the most important case and is adequate to determine the basic sensitivity of the GRS. Peaks were considered for efficiency fitting only if they had sufficient statistical significance and did not overlap substantially with other peaks (including background and escape peaks), with a few exceptions that were well characterized. A total of 51 peaks spread fairly

evenly over the energy range of interest were used in the efficiency fitting, with only 3 significant outliers in the fit. The polynomial degree was chosen to be 6 for the fit. A smaller degree yielded a poorer fit; a larger degree gave no better fit.

In Fig. 14, the calculated efficiency from the experimental calibration data is compared to the GEANT Monte Carlo computation used for the MESSENGER GRS CDR science presentation. The calibration data yields an efficiency that is lower than the Monte Carlo result, by ~ 10% for the 440 keV Na line, ~ 20% for the 847 keV Fe line and 983 keV Ti line, ~ 23% for the 1943 keV Ca line, and ~ 30% for the 6761 keV Ti line and 7646 keV Fe doublet. Note that no attenuation corrections have yet been applied to the calibration data. These corrections are estimated to raise the calibration efficiency by up to 10% for low energies and a percent or so for high energies. The flat slope in the calibration efficiency below 250 keV is an extrapolation and probably is incorrect.

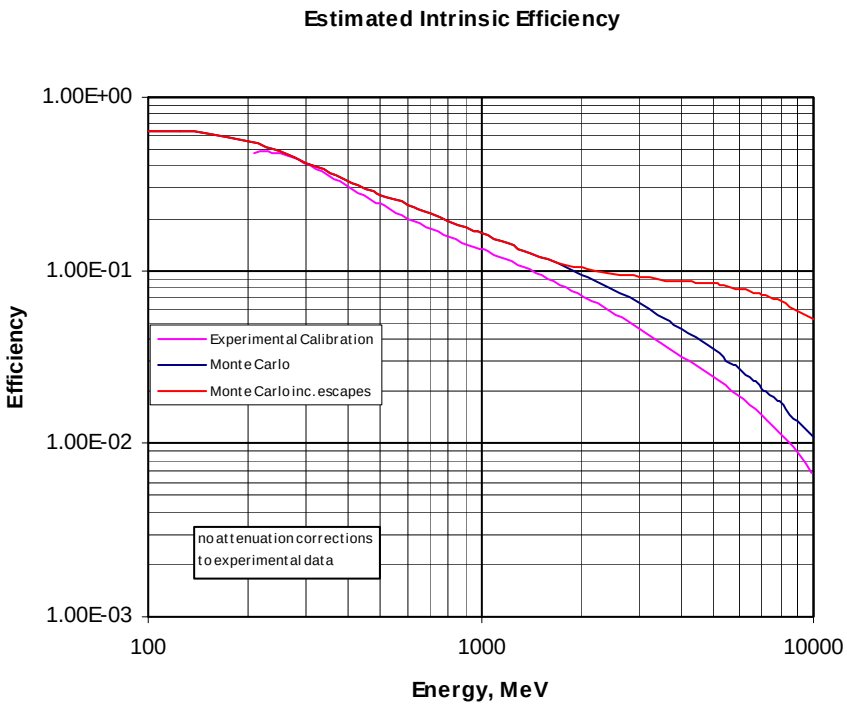


Fig. 14. Comparison of GRS intrinsic efficiency calculated from calibration data and Monte Carlo.

## CROSS CALIBRATION

The gamma-ray spectrometer measures the average bulk elemental composition to a depth of 10-30 cm into the surface material. In space, the gamma-ray emission comes primarily from interactions of cosmic rays. Interactions that lead to crust element identification typically are inelastic scattering and capture of neutrons produced by the cosmic rays in the crust. Unlike composition measurements taken by other instruments, such as X-ray fluorescence and IR reflectance spectroscopy, this technique is insensitive to the surface composition in a very thin surface layer, but is sensitive only to the bulk

composition. Thus, no cross calibration measurements with other instruments that measure Mercury crust composition are feasible or necessary.

## FUNCTIONAL PERFORMANCE

In addition to calibration measurements mentioned in the calibration plan, there are GRS functions that must be adequately performed in order for the spectrometer to meet science mission requirements. The voltage applied to the flight Ge detector must be sufficiently high to fully deplete the semiconductor crystal. The cryocooler must cool the Ge detector to the required operating temperature, reaching temperature stability in a reasonable length of time. The cooler microphone data should have sufficient fidelity to clearly define cooler vibration modes. The anneal heaters must heat up the Ge detector to annealing temperature in a reasonable length of time. The plastic anticoincidence shield should reliably reject on-scale cosmic rays. A comprehensive performance test has been developed to determine that the spectrometer is functioning and performing properly. GRS functional performance during tests related to these issues is briefly discussed in this section.

### Ge crystal high voltage depletion

A plot of the crystal capacitance as a function of high voltage applied to the Ge crystal is shown in Fig. 15. The capacitance curve is observed to begin flattening out at 2200 volts for the flight detector, becoming nearly completely flat at 3000 volts, indicating full depletion at that point. Since the flight detector is operated at 3200 volts, it is fully depleted, and insensitive to small changes in the high voltage. The high voltage supply does not need to be regulated to close tolerance, such as required for photomultiplers.

### Cryocooler microphone

A buffered and filtered version of the preamp output signal is sent to a sampling ADC. A plot of the the relative amplitude in dB of the fast fourier transform of data from this "microphone" circuit is shown in Fig. 16. The data is sampled at a maximum bandwidth of 5 kHz for 6 seconds. The plot goes out to only 2500 Hz, the Nyquist frequency, to avoid aliasing. The fundamental rotation frequency and its harmonics increase with power drawn by the cooler. When the cooler is "working" moderately, it rotates at ~ 60 Hz. Since the stator permanent magnet has 22 segments, the fundamental "electronic" frequency seen in the plot is ~ 1320 Hz. The spectrum is seen to be rich in subharmonics of 60 Hz and intermodulations and other modal frequencies that decrease rather slowly with frequency from the fundamental.

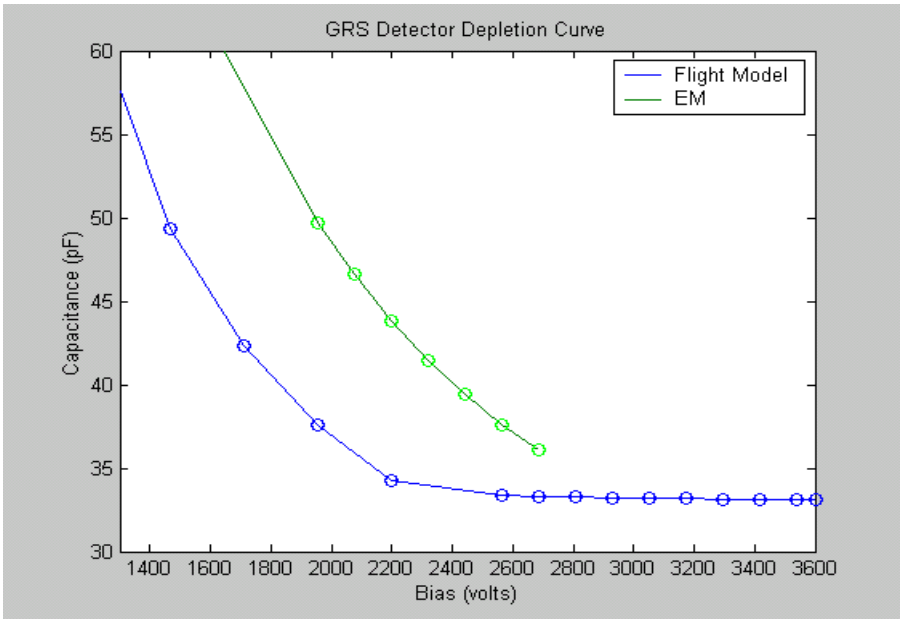


Fig. 15. GRS Ge crystal depletion curve for flight and engineering models.

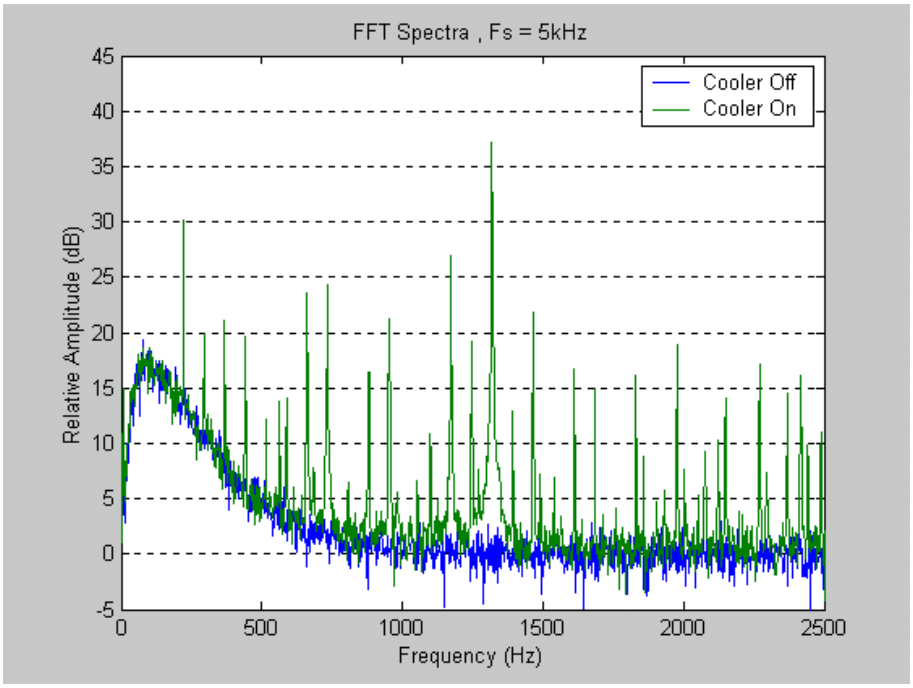


Fig. 16. Cryocooler microphone data sample for flight model GRS.

After the sample was digitally captured by GSEOS, it was played back in analog through a speaker attached to a PC, so the sample could be heard. Although the sampling frequency is slightly too low to sample the first harmonic of the “electronic” fundamental, the sound appeared to the human ear to have good fidelity with the sound heard directly from the same cooler and was judged adequate to detect some sound changes that might indicate bearing noise, presaging cooler failure. However the

background electronic noise generated by cosmic rays striking the detector in space may make it difficult to detect cooler sound nuances.

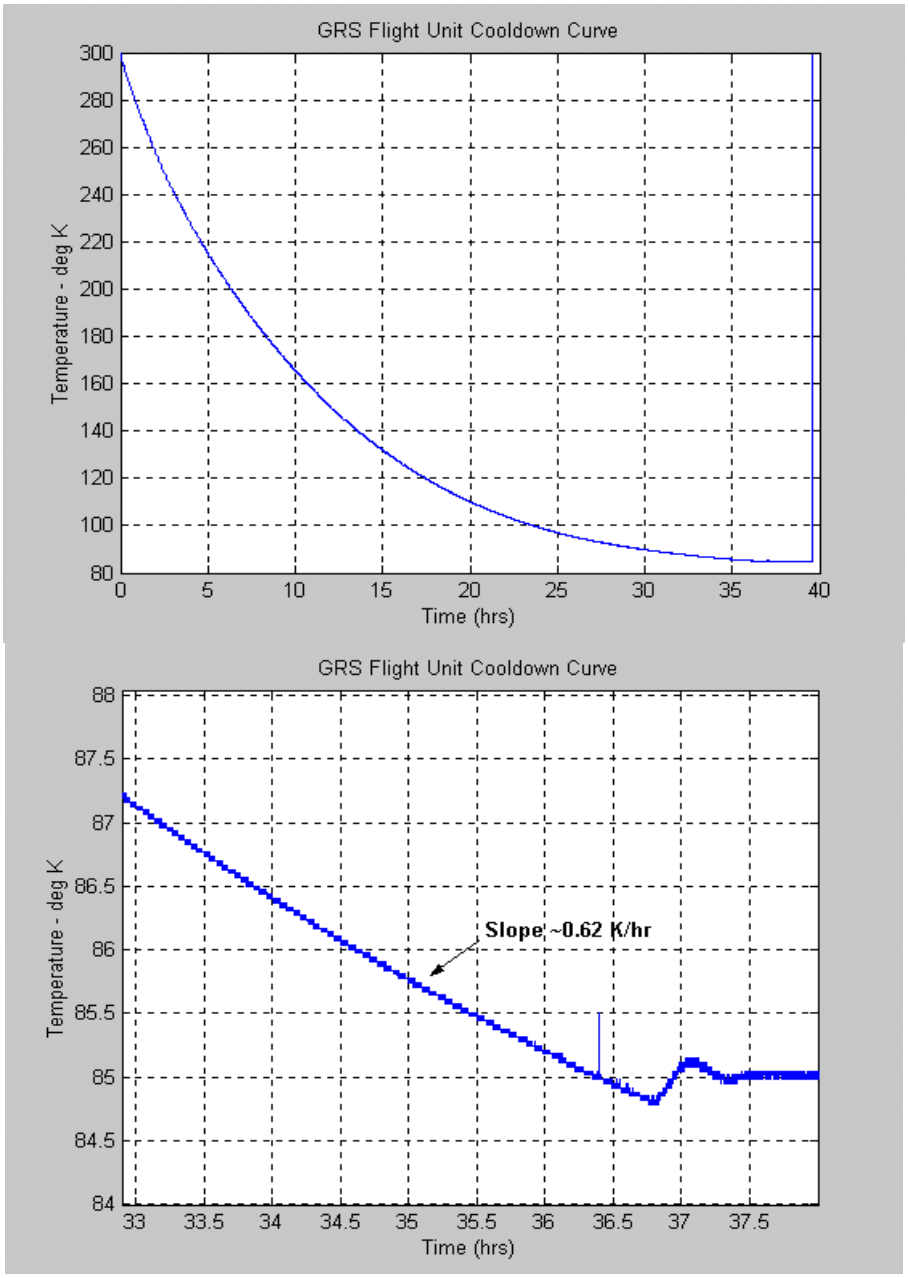


Fig. 17. Ge capsule flight unit cooldown from room temperature to operating temperature.

**Cryocooler cooldown of Ge detector capsule**

The cryocooler cooldown of the Ge capsule from room temperature to 85K operating temperature is shown in Fig. 17. The lower graph shows a time-expanded view of the end of the cooldown. The slope at the end is expected to be proportional to the difference between the cooler heat lift and the capsule total heat load at this point and inversely proportional to the capsule heat capacity. Time required to reach regulation is 37.5 hours.

Fig. 18 shows the corresponding warmup curve for the Ge capsule, if the cooler turns off for some reason. Note that in ~ 1.3 hr, the Ge crystal temperature drifts up to 100K, completely outside the desired operating range due to cosmic ray radiation damage concerns. Going back to Fig. 17 at the 100K point in the cooldown, it is seen that ~ 24 hr is required to bring the Ge capsule back into regulation at 85K, if the cooler is turned back on. The spectrum peaks will be smeared out greatly during this 25.3-hr period by the 185 ppm/K Ge temperature coefficient (unless corrected over small data collection intervals, impossible if not preplanned). During this 25.3-hour period, the cooler will be stressed (lowering its lifetime), the detector will be subject to significantly more radiation damage, and science data sensitivity will be greatly reduced. It is obviously strongly preferable that temperature-regulated cooler operation be maintained continuously in orbit, except for preplanned outages, such as annealing to repair radiation damage.

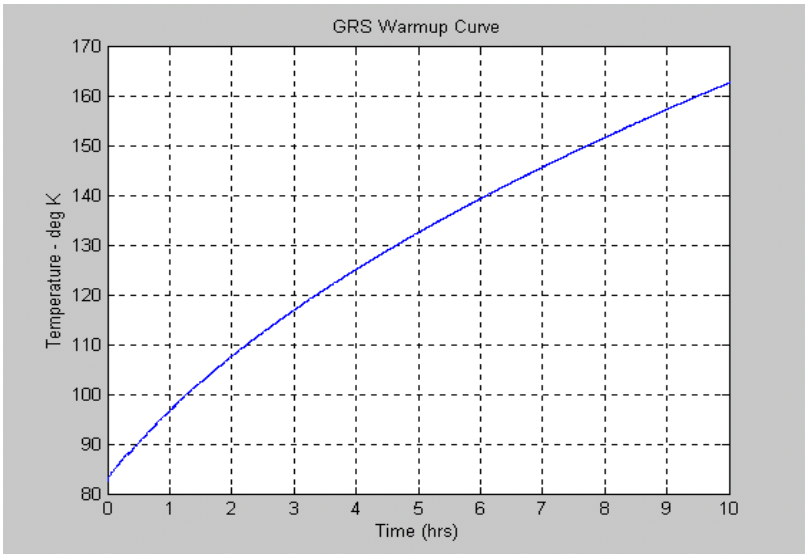

Fig. 18. Ge capsule warmup from operating temperature after cooler turnoff.

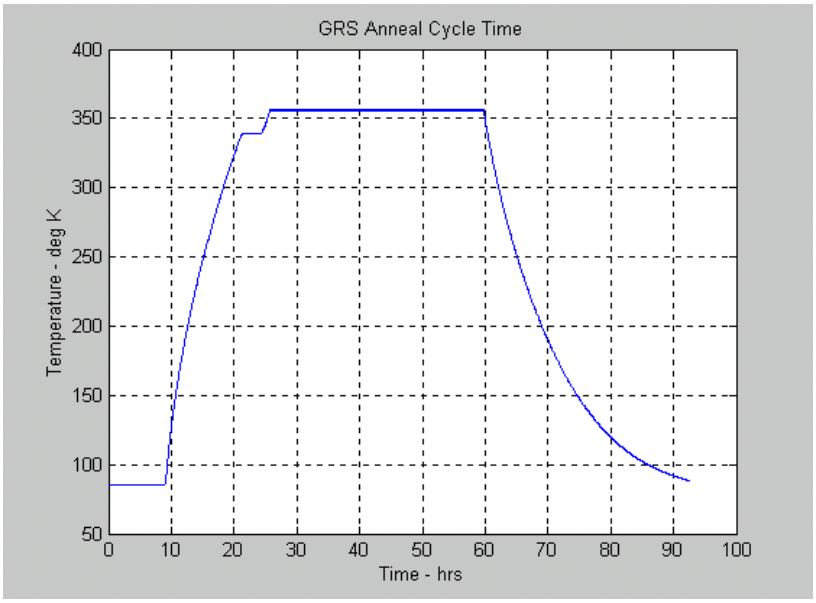

Fig. 19. Ge capsule anneal cycle after cooler turnoff.

| FSCM NO. | SIZE | DRAWING NO. | REV. |
|---|---|---|---|
| 88898 | A | 7384-9466 | A |
| SCALE | DO NOT SCALE PRINT | SHEET 28 of 34 | |

**Relative light output from anticoincidence shield**

The light path from the upper portion of the cylindrical upper side shield to the PMT is relatively long and must pass through the bottom endcap shield. Sufficient light must be received for each traversing cosmic ray depositing on-scale energy, at a lower level discriminator setting above the noise, to detect the event. If light from such events in the bottom shield is much stronger than that from other shield portions, the other events will be lost. In Fig. 20, a collimated $^{137}$Cs source is used to examine the relative light output from shield portions at different heights. All three levels of the side shield yielded Compton edges ending at ~ channel 70, while the Compton edge for the bottom shield ends at ~ channel 160, a factor of 2.3 higher. With the LLD setting available, this variation is quite sufficient to detect all on-scale cosmic rays.

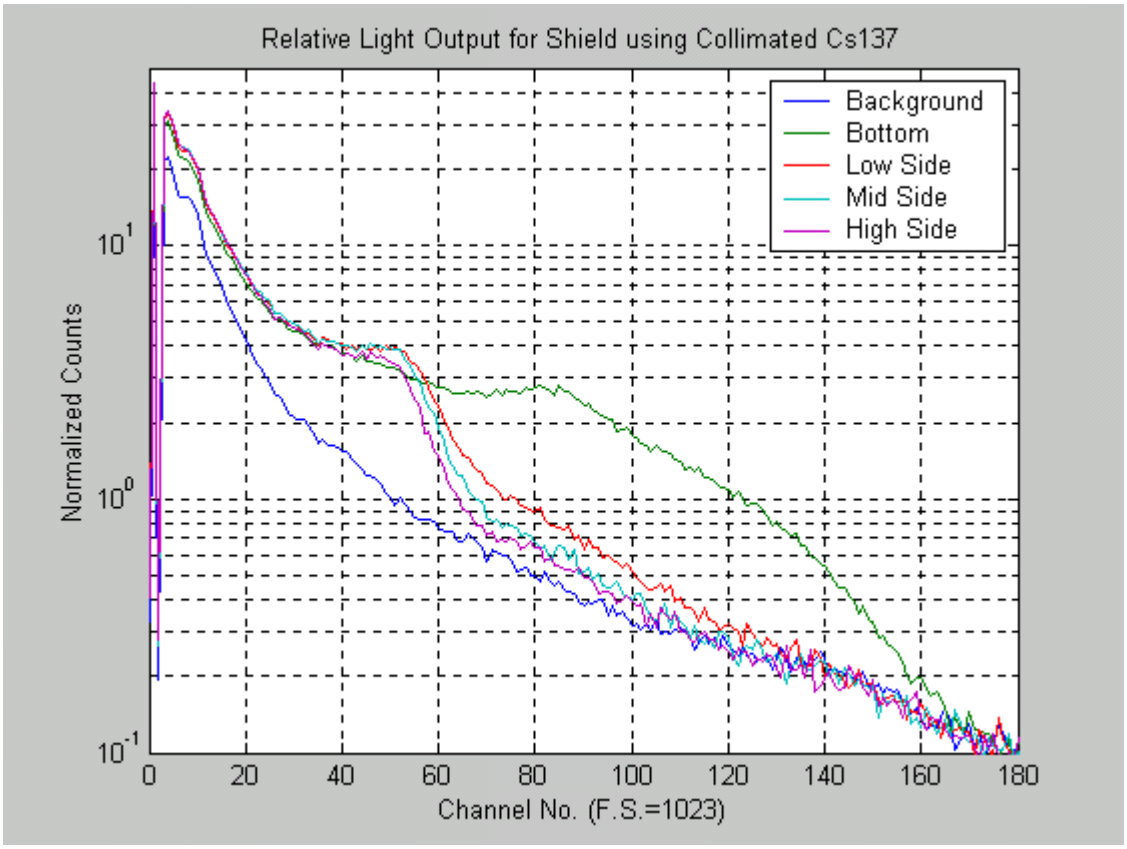


Fig. 20. Relative light output at different heights of the anticoincidence shield.

**Comprehensive performance test**

The test suite mentioned below was devised to test the functionality and performance of the flight GRS. Items tested include cooldown time and power during temperature regulation, HPGe leakage current, energy scale, and energy resolution, pulser resolution, and anticoincidence shield background and signal response and neutron rejection. Typical values measured during the test are given below and uniformly exceed the test specifications.

1. The GRS shall be able to cool down the HpGe detector to an operating temperature of 85K in a period not to exceed 40 hours under room temperature conditions.

   Time = 38 hrs. 22 min. to first crossing. Stator temperature = 29.1C

2. Once in regulation at 85 K, the cooler shall not draw in excess of 850 mA @ 15V.

   Peak current = 794 mA. Equilibrium current = 732 mA.

3. The leakage current for the HpGe detector biased to 3200V shall be less than 100pA.

   Calculated leakage current = 6 pA, after correction for a 102 pA dc offset and a signal current of 80 pA (Co-60 @ 2.6kHz, mean energy=568.6keV).

4. The energy resolution of the HpGe detector biased to 3200V shall be less than 3.6keV FWHM @ 1332 keV for count rates less than 3 kHz.

   3.49 keV FWHM @ 1332 keV, net counts = 130,700, count rate = 631 Hz.

   6.51 keV FWTM

5. The energy resolution on the internal pulser line (7.9 MeV) shall measure less than 3.2keV FWHM.

   3.11 keV FWHM @ 7986 keV, net counts = 44,400, pulser rate = 7.6Hz. 5.72 keV FWTM

6. The energy scale for the HpGe channel shall be 0.605 keV/ch +/- 1%. The energy offset for the HpGe channel shall be 0 keV +/- 1.5keV.

   E = 0.605344 keV/ch – 1.121 keV

7. The background counts for the Shield channel in the absence of a source shall be less than 200 cps at an operating voltage of 600V.

   167 cps @ 600V.

8. At an operating voltage of 600V, the Shield channel spectrum shall show a broad peak near channel 50 when exposed to Cs-137 and a comparable peak near channel 100 when exposed to Co-60.

   Cs-137 peak = ch 48, count rate = 3kHz.

   Co-60 peak = ch 99, count rate = 2.6 kHz.

9. The anti-coincidence system shall demonstrate approximately a 3:1 rejection of the 478 keV line when exposed to AmB.

   HpGe Raw counts: gross = 1650, net = 635, ROI = 470-484 keV.

   HpGe A-C counts: gross = 920, net = 170, rejection ratio = 3.7:1

## CONCLUSION

All necessary GRS tests and calibrations have been conducted. Sufficient data has been analyzed to determine mission readiness. The measured DNL of the GRS flight unit is quite small and devoid of any systematic trends. It exceeds the 3 sigma goal of 1% of a channel. No spectral corrections need to be applied. The measured flight electronics INL spread over the spectrum is less than 2 channels and the change over the full temperature range is a channel or less, so the INL spread and change over any orbit is negligible. Again no corrections need to be applied.

The overall electronics offset is only a small fraction of a channel over the full temperature range and can be ignored. However the gain change with temperature of each electronic component must be corrected in flight by knowing the temperature coefficients and measured temperatures on instrument components. Although temperature coefficients of all electronic components can be determined from the data taken in thermal vacuum tests, this data has not yet been analyzed. However climate chamber tests indicate maximum gain drifts of ~ 95ppm/K for the preamp and ~ 20 ppm/K for the remainder of the electronics, so such gain drifts will yield only small spectral corrections.

Although TV test data on the pulser peak shift with temperature remains to be analyzed, the pulser has been stable in climate chamber tests, with excellent energy resolution. The measured Ge detector energy resolution over the energy range of interest during the spacecraft CPT test was excellent, exceeding the 4 keV goal at 1332 keV. Although the TV test data on energy resolution has not yet been analyzed, essentially no dependence on temperature is expected. The low level discriminator settings for the Ge detector and anticoincidence shield have been determined, easily exceeding the noise levels while detecting the lowest amplitude signal desired.

The functional test results also indicate more than adequate performance for the GRS to meet science mission requirements. The voltage applied to the flight Ge detector is more than sufficient to fully deplete the semiconductor crystal. The cryocooler cools the Ge detector to the required operating temperature, reaching temperature stability in a reasonable length of time. The cooler microphone works and provides sufficient fidelity (at least on earth). The anneal heaters heat up the Ge detector to annealing temperature in a reasonable length of time, with power to spare. The plastic anticoincidence shield is expected to reliably reject on-scale cosmic rays. The spacecraft GRS comprehensive performance test data uniformly exceeds the goals set for the GRS.

The GRS spatial calibration performed at the NIST cold-neutron-beam reactor holds the promise for a new higher level of calibration precision for this space-borne Ge gamma-ray spectrometer, while requiring far less total measurement time than needed for Ge spectrometers in prevous missions. However some tedious attenuation data corrections are required that have not yet been done. The efficiency calculation from the experimental data has been performed only for the nadir-pointing case with no escapes, with some small attenuation corrections not yet done, but this is the most important case. This efficiency is adequate to determine the basic spatial performance of the GRS.

Shown in Fig. 21 is the MESSENGER Ge GRS CDR slide depicting sensitivities to elements of Mercury's crust that are considered important for describing planetary evolution, based on a GEANT Monte Carlo Ge detector model. Red vertical lines indicate element signals expected for evolutionary

models (indicated by triangles along the lines). If a red line appears above the lowest black curve, that gamma-ray signal will be measurable to the 3-sigma level or better for 137 hours of observation time at low altitude (137 hours is the estimate of the total mission observation time at low altitude). If a red line appears above the lowest blue curve, that gamma-ray signal will be measurable for only 8 hours of observation time at low altitude (8 hours is expected to allow coarse mapping of the associated element).

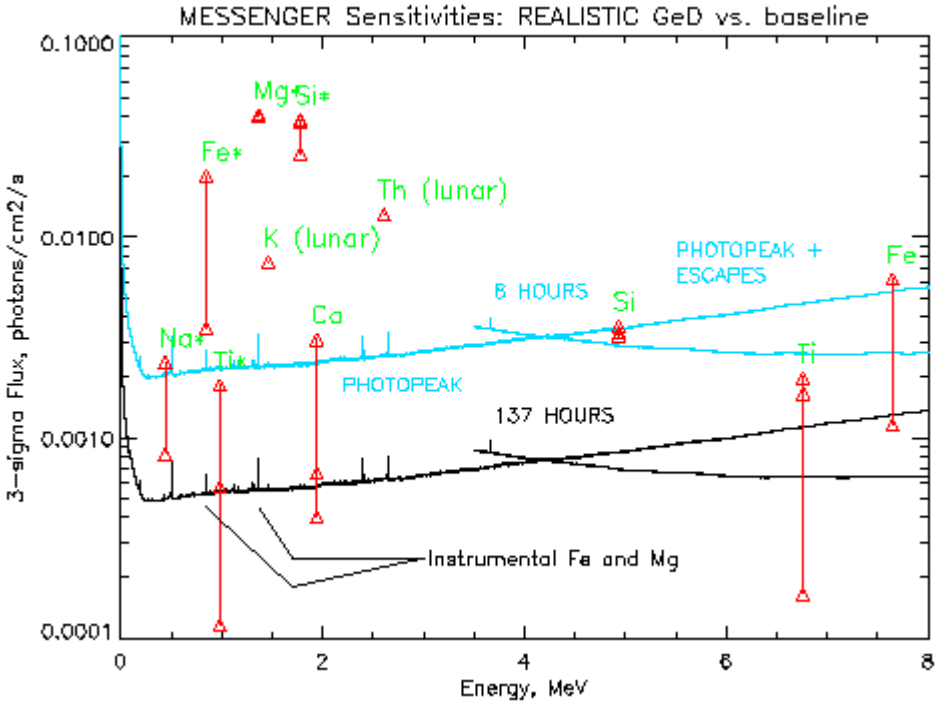


Fig. 21. Ge GRS sensitivity to gamma-rays from elements of Mercury's crust.

When the calculated efficiency from the experimental calibration data is compared to the Monte Carlo computation, the calibration data yields an efficiency that is lower than the Monte Carlo result, by ~ 10% for the 440 keV Na line, ~ 20% for the 847 keV Fe line and 983 keV Ti line, ~ 23% for the 1943 keV Ca line, and ~ 30% for the 6761 keV Ti line and 7646 keV Fe doublet. The red lines for these gamma-rays are lowered by these percentages on the graph. The only CDR conclusion that is changed is that Ca cannot be mapped and can be measured for only one of the three evolutionary models. Fe, Mg, Si, K, and Th should still be mappable, Na should still be measurable, and Ti should still be measurable for two evolutionary models. The scientific objectives of the GRS component of the GRNS instrument (defined in the Introduction) are expected to be met and exceeded: (1) provide surface abundances of major elements, particularly those elements whose abundances are thought to be indicative of planetary evolution; (2) provide surface abundances of Fe, Si, and K and infer alkali depletion from K abundance; (3) map surface element abundances where possible, otherwise provide surface-averaged abundances or establish upper limits.

**APPENDIX: ACRONYM DEFINITIONS**

ADC - Analog-to-Digital Converter
DNL - Differential Non-Linearity
EPU – Event Processing Unit
ETE - End-To-End
FWHM – Full Width at Half Maximum
FWTM – Full Width at Tenth Maximum
Ge - germanium
GRNS – Gamma-ray Neutron Spectrometer
GRS - Gamma-ray Spectrometer
GSE - Ground Support Equipment
GSH - Gamma Sensor Head
HP – High purity
INL – Integral Non-Linearity
LLD - Lower Level Discriminator
LN2 – Liquid Nitrogen
MCA - Multi-Channel Analyzer
MO - Mars Odyssey
PDS – Planetary Data System
PMT – Photomultplier Tube
PVT - Polyvinytoluene
SOC – Science Operations Center
TV – Thermal Vacuum
XGRS – X-ray & Gamma-ray Spectrometers

| FSCM NO. | SIZE | DRAWING NO. | REV. |
|---|---|---|---|
| 88898 | A | 7384-9466 | A |
| SCALE | DO NOT SCALE PRINT | SHEET 34 of 34 | |